Sedimentology (1999) **46,** 279–301

Physical and biological controls on the formation of carbonate and siliciclastic bedforms on the north-east Brazilian shelf

VIVIANE TESTA* and DANIEL W. J. BOSENCE†
**CPGG – Universidade Federal da Bahia, Campus Universitário Ondina, Salvador, Bahia, 40170–290 Brazil (E-mail: vtesta@pppg.ufba.br)*
†Department of Geology, Royal Holloway University of London, Egham, Surrey, TW20 0EX, UK

ABSTRACT

The continental shelf of the State of Rio Grande do Norte, Brazil, is an open shelf area located 5°S and 35°W. It is influenced by strong oceanic and wind-driven currents, fair weather, 1·5-m-high waves and a mesotidal regime. This work focuses on the character and the controls on the development of suites of carbonate and siliciclastic bedforms, based on Landsat TM image analysis and extensive ground-truth (diving) investigations. Large-scale bedforms consist of: (i) bioclastic (mainly coralline algae and *Halimeda*) sand ribbons (5–10 km long, 50–600 m wide) parallel to the shoreline; and (ii) very large transverse siliciclastic dunes (3·4 km long on average, 840 m spacing and 3–8 m high), with troughs that grade rapidly into carbonate sands and gravels. Wave ripples are superposed on all large-scale bedforms, and indicate an onshore shelf sediment transport normal to the main sediment transport direction. The occurrence of these large-scale bedforms is primarily determined by the north-westerly flowing residual oceanic and tidal currents, resulting mainly in coast-parallel transport. Models of shelf bedform formation predict sand ribbons to occur in higher energy settings rather than in large dunes. However, in the study area, sand ribbons occur in an area of coarse, low-density and easily transportable bioclastic sands and gravels compared with the very large transverse dunes in an offshore area that is composed of denser medium-grained siliciclastic sands. It suggests that the availability of different sediment types is likely to exert an influence on the nature of the bedforms generated. The offshore sand supply is time limited and originates from sea floor erosion of sandstones of former sea-level lowstands. The trough areas of both sand ribbons and very large transverse dunes comprise coarse calcareous algal gravels that support benthic communities of variable maturity. Diverse mature communities result in sediment stabilization through branching algal growth and binding that is thought to modify the morphology of dunes and sand ribbons. The occurrence and the nature of the bedforms is controlled by their hydrodynamic setting, by grain composition that reflects the geological history of the area and by the carbonate-producing benthic marine communities that inhabit the trough areas.

Keywords Bedforms, carbonate shelf, current-dominated, north-east Brazil, sand ribbons.

INTRODUCTION

Considerable work has been undertaken on the flow dynamics and formation of siliciclastic bedforms on shallow marine shelves (Allen, 1968, 1985; MacCave, 1971; McLean, 1981; Stride, 1982; see also Ashley, 1990). Similar structures are also formed on shallow carbonate shelves (e.g. Farrow *et al.*, 1979; Hine *et al.*, 1981; Wilson, 1986; Shinn *et al.*, 1990), but these have not been

studied in such detail. Bedforms generated on carbonate shelves are more complex than their siliciclastic counterparts due, in part, to the variability in shape, structure and density of carbonate grains (Jell & Maxwell, 1965; Maiklem, 1968; Braithwaite, 1973; Steidtmann, 1982; Flemming, 1992; Prager *et al.*, 1996) and in part to their interaction with carbonate-producing benthic communities (Farrow *et al.*, 1979; Wilson, 1982; 1988).

This paper focuses on describing and interpreting the zonation of shelf sediments and associated bedforms that occur in an open ocean-facing, high-energy shelf off the north-east coast of Brazil. The work is partly based on large-scale Landsat TM images, which enable us to map the morphology and occurrence of the large-scale bedforms, and partly on detailed diver observations and sampling of bedforms, sediments and their benthic communities. An inshore bioclastic sand ribbon zone is described, together with a more offshore zone of very large transverse siliciclastic dunes with stabilized carbonate gravel troughs. These large-scale bedforms appear to be in equilibrium with the high-energy, longshore unidirectional oceanic/tidal currents, seasonally intensified by south-easterly winds, but are also continuously modified by onshore-directed oscillatory wave currents.

The work is descriptive in its approach and is the first detailed study of the area. The combination of Landsat-based seafloor mapping and diver transects enables both the large-scale bedforms and the minor structures to be described and interpreted. This observational approach allows a study of the interactions between the marine benthic communities and the current-generated bedforms. The growth of the two main producers of carbonate sediments, free-living coralline red algae and *Halimeda*, are shown to exert an influence on the origin and on the development of the large-scale bedforms.

This part of the Brazilian shelf is unusual in having both an inshore and an offshore sand supply to a shallow shelf that is mainly accumulating carbonate sediment today. This results in a complex interplay between siliciclastic and carbonate sediments. The controls on the origin of the large-scale bedforms is shown to be related in part to the sea-level history and clastic sediment supply, in part to the high hydrodynamic energy and in part to the carbonate-producing and -stabilizing benthic communities. This is a more complex picture than that presented for siliciclastic shelves, where there appears to be a more straightforward relationship between bedform types and hydraulic energy.

Studies on shelf processes and sediment dynamics are of growing interest in Brazil, as the mineral resources of the continental shelf are currently being re-evaluated. The Brazilian continental shelf stretches some 6000 km from 4°N to 35°S (Campos *et al.*, 1974). Almost half of the shelf area is covered by biogenic carbonate, and it represents one of the longest carbonate depositional environments in the world (Alexandersson & Milliman, 1981; Carannante *et al.*, 1988). Previous work has shown that the middle (20–40 m water depth) and outer (>40 m water depth) shelf are dominated by carbonate sediments (>75%), in contrast to the inner (<20 m water depth) shelf, which was previously believed to be siliciclastic rich (<25% carbonate) (França *et al.*, 1976). In certain areas, such as portions of the Pernambuco shallow shelf, Coutinho (1981) stated that carbonate sediments form a more continuous blanket from the inner to the outer shelf. The Rio Grande do Norte shelf area is another in which carbonate sediments extend from depths as shallow as 5 m (Testa *et al.*, 1994; Testa, 1996a; Testa & Bosence, 1998) and cover over two-thirds of the shelf area above the wave base.

The present study area was chosen for a pilot study because of the extraordinarily high light penetration of shelf waters shown in band 1 on Landsat TM images. This enables mapping of large-scale seabed structures down to depths greater than 35 m Fig. 1) at a scale of 1:50 000 (Vianna *et al.*, 1991). An area of 500 km^2 was mapped, and six shoreline-parallel sedimentary zones were redefined from previous work in the area conducted by Vianna *et al.* (1991).

ENVIRONMENTAL SETTING

The study area is located offshore from the fishing towns of Touros and Rio do Fogo in the state of Rio Grande do Norte, Brazil (Fig. 1). It is an open, ocean-facing, shallow shelf with no bays. The coast is dominated by vegetated siliciclastic aeolian sand dune fields and associated lagoons.

The area experiences a seasonal warm and semi-arid tropical climate. The more western areas are distinctly arid. The summer is dry and may last 6–7 months (September to February). The winter (March to August) has a higher rainfall, with peaks in March and April (Rao *et al.*, 1993). Annual rainfall is 600 mm per year

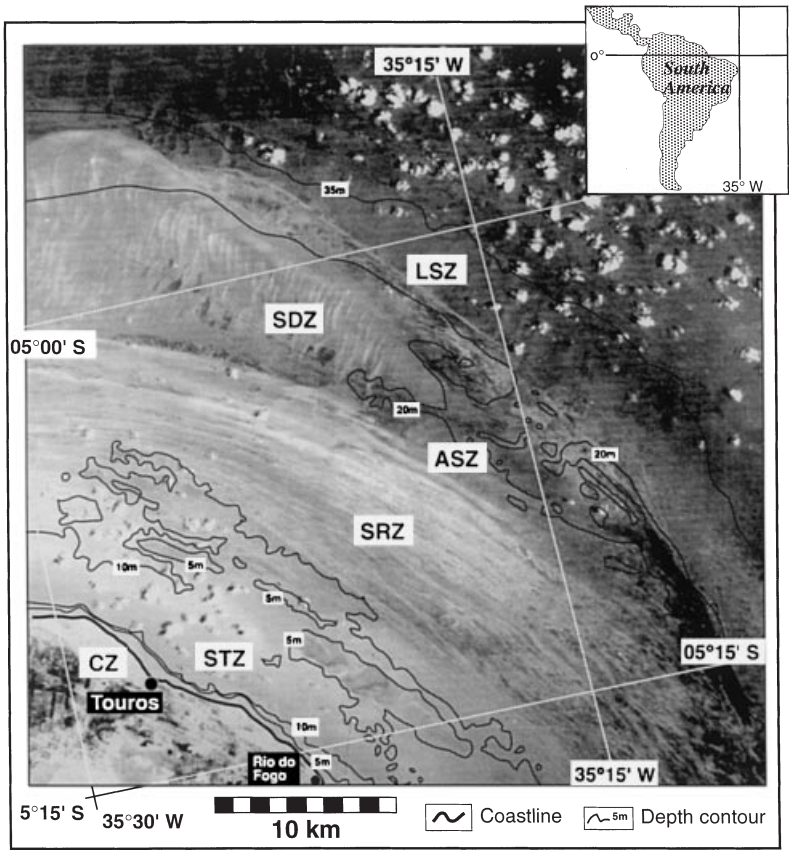

Fig. 1. View of study area as imaged in Landsat TM, band 1 with coastline in south-western corner. The area where the seafloor is imaged corresponds to the inner shelf (above wave base). The main zones are: coastal zone (CZ), sublittoral turbid zone (STZ), sand ribbon zone (SRZ), algal stabilized zone (ASZ), subaqueous dune zone (SDZ) and lithified sediment zone (LSZ). Zone boundaries are shown in Fig. 2.

(Rao *et al.*, 1993), occasionally exceeding 1500 mm per year (Andrade, 1964; Schultz *et al.*, 1992). The seasonality is related to the east–west movement of high pressure in the tropical Atlantic (Tchernia, 1980).

Sea-surface temperatures recorded over a period of 30 years show a range from about 26·5°C in the winter to about 28·5°C in the summer (Servain *et al.*, 1990). Coupled with the temperature, the salinity is also typical of a tropical environment and varies between 36‰ and 37‰ (Laborel, 1969; França *et al.*, 1976).

The west Atlantic has the clearest waters of the tropical Atlantic ocean (Sorokina, 1984). The waters off north-east Brazil are nutrient depleted with a low suspended sediment concentration of 0·25 mg L^{-1} (Emery & Milliman, 1975; França *et al.*, 1976). High water clarity is found in the offshore shallow shelf area of Rio Grande do Norte state, where mapping of sea bottom features is possible using passive remote-sensing techniques down to 35 m water depth (Vianna *et al.*, 1991).

There are few rivers discharging suspended sediments or increased levels of nutrients to promote the growth of phytoplankton in the area. However, a small plankton bloom lasting 2–3 days was observed approximately 15 km offshore in March 1992, which may relate to sporadic bursts of low temperature caused by offshore air circulation patterns (M. L. Vianna, personal communication). Field observations and Landsat images show that water turbidity may increase locally in coastal areas because of the remobilization of fine sediments mainly from reef areas. Turbid plumes of fine sediments are seen on Landsat images to be transported by longshore currents towards the north-west. Periods of strong winds and spring tides also produce water turbulence, and associated turbid waters can extend up to 15–20 km offshore (between 15 and 20 m water depth).

There are no available data on the amount and composition of suspended sediments in the area.

Ocean currents

The north-east Brazilian shelf lies within the ambit of the North Brazil current, which has its origins in the southernmost part of the South Equatorial Current (SEC). The SEC flows westwards and impinges on the north-eastern promontory of South America, at approximately 10°S, where it bifurcates (Peterson & Stramma, 1991).

The Brazil Current (BC) flows southwards and separates from the coast at 12°S (Stramma *et al.*, 1990). The other branch, comprising 75% of the SEC, forms the North Brazil Current (NBC) at 7°S and flows to the north-west (Stramma *et al.*, 1990; da Silveira *et al.*, 1994). The subsurface core of the NBC is found between 100 and 150 m water depth and is characterized by relatively high salinity (>37‰) (da Silveira *et al.*, 1994), and near-surface current velocities vary from 30 cm s^{-1} (February) to 40 cm s^{-1} (August) (Richardson & Walsh, 1986; Peterson & Stramma, 1991). The accumulation of water derived from residual tropical circulation in easternmost Brazil also generates longshore currents, which flow north-west with the NBC (Richardson & Walsh, 1986). There are no published measurements of near-bed water velocities from the study area.

Tides

The area experiences a semidiurnal upper mesotidal to lower macrotidal (Hayes, 1979) regime with a maximum tidal range of 3·8 m (Mabessone & Coutinho, 1970; Brazilian Navy charts). There are no published records of tidal current speed or direction within the region. Spring tides and strong winds are combined at times of full moon, and it is well known by local fishermen and from diving observations that these lunar phases generate strong currents with increased water turbidity in areas less than 15–20 m deep. This depth interval is situated some 15–20 km offshore. Tidal currents are so strong that diving can only safely be carried out during the 2–4 h of slack water. Outside this period and during the whole period of spring tides, diving work is unsafe, and water velocities are believed to be well in excess of 100 cm s^{-1}.

Winds and waves

Waves are believed to be important contributors to the high hydrodynamic energy of the environment, and wave-generated currents are commonly seen while diving to move surface sediments. Accurate wave measurements are not available, but wave heights were estimated during dives in fair weather conditions to be approximately 1–1·5 m in approximately 16 m of water depth. Wave-generated bedforms are recorded throughout the area down to 23 m water depth.

The change from the wet to the dry season (July to September) is accompanied by variations in regional wind strength caused by the seasonal movement of the high pressure centre from the west to the east of the tropical Atlantic Ocean (Tchernia, 1980). South-easterly trade winds predominate throughout the area with a minimum velocity of 3·6 m s^{-1} during April and a maximum velocity of 6·8 m s^{-1} during August (Servain *et al.*, 1987). The magnitude of these winds is increased by the northward movement of the Intertropical Convergence Zone (ITCZ) (Molinari *et al.*, 1986). The ITCZ movement influences both the NBC and the longshore current velocity seasonally (Molinari *et al.*, 1986). Both of these currents, as well as the trade winds (see Molinari *et al.*, 1986), have higher velocities from April to June (Richardson & Walsh, 1986). These increased wind-forced currents were observed to increase water turbidity in the study area, particularly when combined with storms and spring tides (see above).

METHODS

The inner continental shelf of Rio Grande do Norte is poorly known and, although Landsat images have been used to provide a broad description of the area, this is the first work that provides detailed mapping of these images (Figs 1 and 2), followed by extensive ground truthing by diving (for details, see Testa, 1996). The first investigations in this area were reported by Solewicz (1989), Vianna *et al.* (1991), Cabral (1993) and Vianna *et al.* (1993), who showed the advantages of using Landsat TM imagery to assess large-scale sea-bottom features and their possible relationship with bathymetry.

The present survey is partly based on Landsat TM imagery (Solewicz, 1989; Vianna *et al.*, 1991), which was used to map out zones of the inner shelf on the basis of bedform morphology using grey levels in band 1 (0·45–0·52 μm). When comparing the bedforms with images obtained from ship-based oceanographic investigations, it is important to realize that the scale of the satellite images (Fig. 1) is much larger (e.g. 1:50 000) than the scale of side-scan sonar images (commonly 1:200; Flemming, 1976). The overall shapes of the large-scale bedforms are clearly visible on the satellite images, depending on the reflectance contrast, and have a theoretical resolution of one pixel (30 m across). The coordinates of the sites were plotted before the field work using Geographical Information Systems

(GIS), and field site co-ordinates were acquired using a global positioning system (GPS).

Fieldwork was carried out in March–April 1992 and January–February 1994. Five transects were selected in order to cover a large range of grey levels of the Landsat TM image as a reflection of the variation of the sea bottom composition. Diving was undertaken at 110 sites, of which 26 focused on the sampling and measurement of previously located bedforms (Fig. 2). The large-scale bedforms were studied by either single dives across each bedform (i.e. the transverse dunes) or a series of dives (three or four) along transects across structures (i.e. sand ribbons). The height of the large-scale bedforms was obtained by recording the water depth on the depth gauge during dives, whereas their spacing was obtained using the Landsat TM image. Height and spacing of small-scale bedforms were measured directly while diving. The orientation of the large-scale bedforms was obtained from the Landsat image, and small-scale bedforms were oriented using an underwater compass. The present dataset includes the composition and texture of the sediments, measurements of height, spacing and morphology of bedforms, descriptions of their setting and underwater photographs of representative features.

Sediments were collected with a scoop and sieved at 1-phi intervals, and bulk samples were resin impregnated. Acetate peels were made for point counting ($n = 400$) for compositional analysis.

The study area has a variety of bedforms, which range from kilometres to tens of centimetres in scale; they are also variable in shape and composition. To assess their characteristics, the criteria used to describe the large current-formed bedforms follows those suggested by Ashley (1990); namely, the environment of formation of the bedform, its height, spacing, morphology, superposition of bedforms, sediment texture and composition. Wave-formed structures are described as large wave ripples for those with a spacing greater than 60 cm, whereas smaller spaced structures were simply described as small wave ripples.

All large- and small-scale bedforms described in this paper are considered to be in equilibrium with the present-day hydrodynamic energy regime. Therefore, the term superposition is used here, instead of superimposition, which refers to younger bedforms resulting from a more permanent change in the hydraulic regime (Jackson, 1975).

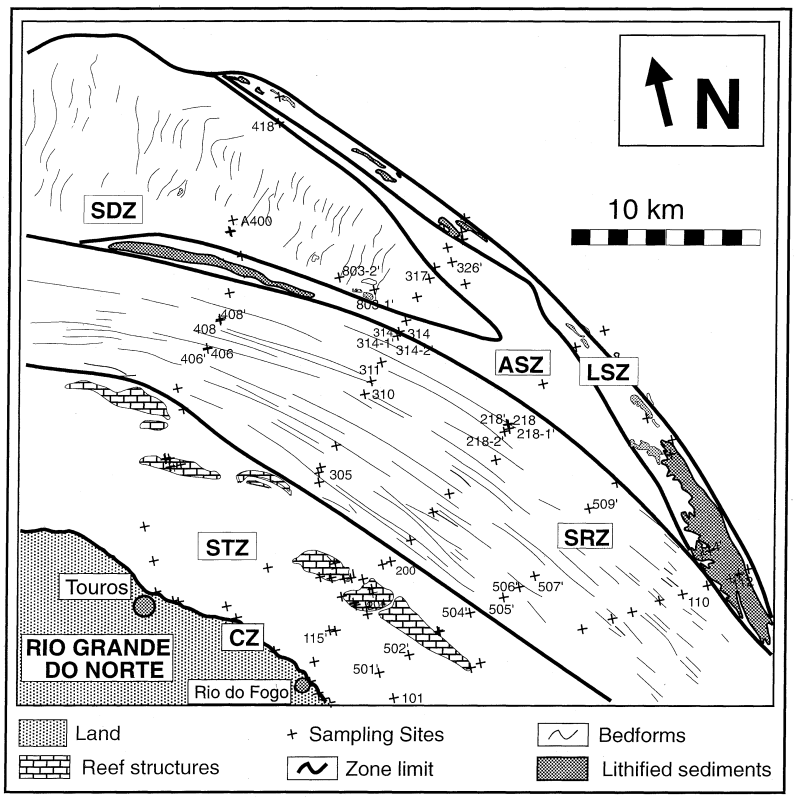

Fig. 2. Map of the large-scale sedimentary and biogenic features in the study area, based on the Landsat image (see Fig. 1). Sampling sites, marked by crosses, were obtained in two field seasons carried out during March–April 1992 and January–February 1994, and are referred to in the text and in Tables 1 and 2.

IMAGE INTERPRETATION AND INNER SHELF ZONATION

The Landsat image analysis, the diver transects and the sediment analysis allows the region to be divided into six main sedimentary zones (Table 1). These zones are approximately parallel to the present-day coastline and inner shelf margin (Figs 1 and 2).

Coastal zone (CZ)

This zone has a relatively narrow siliciclastic beach (Fig. 3A), with rippled and plane laminated sands, although transverse sand cusps may occur during spring tides. Rhodoliths (free-living forms of crustose coralline red algae), reworked from the sublittoral areas, are commonly found on the beaches. Large (1–10 km long and 5–50 m high) aeolian dunes of medium- to fine-grained siliciclastic sand (<5% carbonate grains) occur landward of the beaches. These dunes are longitudinal features oriented NE–SW with the steep avalanche faces pointing to the NE. Inland lagoons fringed by dense vegetation are common in interdune areas. The siliciclastic sand beaches are locally carbonate cemented to form beachrocks in the upper intertidal zone. Average ^{14}C dates of mollusc shells found within beachrocks from the region range from 6735 years BP to 4915 years BP (Oliveira *et al.*, 1990; E. Bagnoli, personal communication). Pleistocene grainstones, packstones and Tertiary sandstones form small cliffs (Srivastava & Corsino, 1984), whose fragments are commonly found reworked within modern beach sediments.

Sublittoral turbid zone (STZ)

This 8- to 9-km-wide zone parallels the shoreline and is subjected to intense sediment resuspension, resulting in turbid coastal waters. Nevertheless, it is only in this zone that coral patch reefs occur. These are up to 6 km long and 2 km wide (Figs 1 and 3B) and appear as elongate grey shapes in the Landsat image (Figs 1 and 2). Buried reefs, apparently related to Holocene lower sea-level stands (see Testa, 1996, 1997) appear on the Landsat image as well-defined elongated grey areas (Fig. 1). Reefs are mainly built by *Siderastrea* and *Millepora* in association with crusts of crustose coralline algae (*Lithophyllum* and *Mesophyllum*) (Testa, 1996, 1997).

Between the coast and the patch reefs are localized occurrences of reworked *Halimeda*-rich sands and seagrass. Here, symmetrical large wave ripples (see Tables 1 and 2, sites 101 and 105) and small wave ripples occur. Three-dimensional

Table 1. Shallow shelf zones: their bedforms and characteristics.

Setting	Large-scale feature	Small-scale feature	Nature of sediments	Carbonate percentage
Coastal zone	Beaches, beachrock, sand cusps, aeolian dunes	Ripples	Siliciclastic sands	< 13
Sublittoral turbid zone	Coral patch reefs, buried reefs	Ripples	Bioclastic carbonate sand	> 90
Sand ribbon zone	Sand ribbons	Ripples	Bioclastic carbonate gravelly sand	30 to > 90
		Large ripples	Bioclastic carbonate	50 to > 90
Subaqueous dune zone	Very large transverse dunes	Large ripples	Siliciclastic and bioclastic carbonate sands	6 to > 90
	Sand plain	Transverse and longitudinal ripples	Siliciclastic sands	< 6
Stabilized algal zone	Algal growth bed	Coralline algal framework	Bioclastic carbonate gravelly sand	60 to > 90
Lithified sediment zone	Submerged sandstone outcrop	Ripples	Bioclastic carbonate and siliciclastic sand	> 80

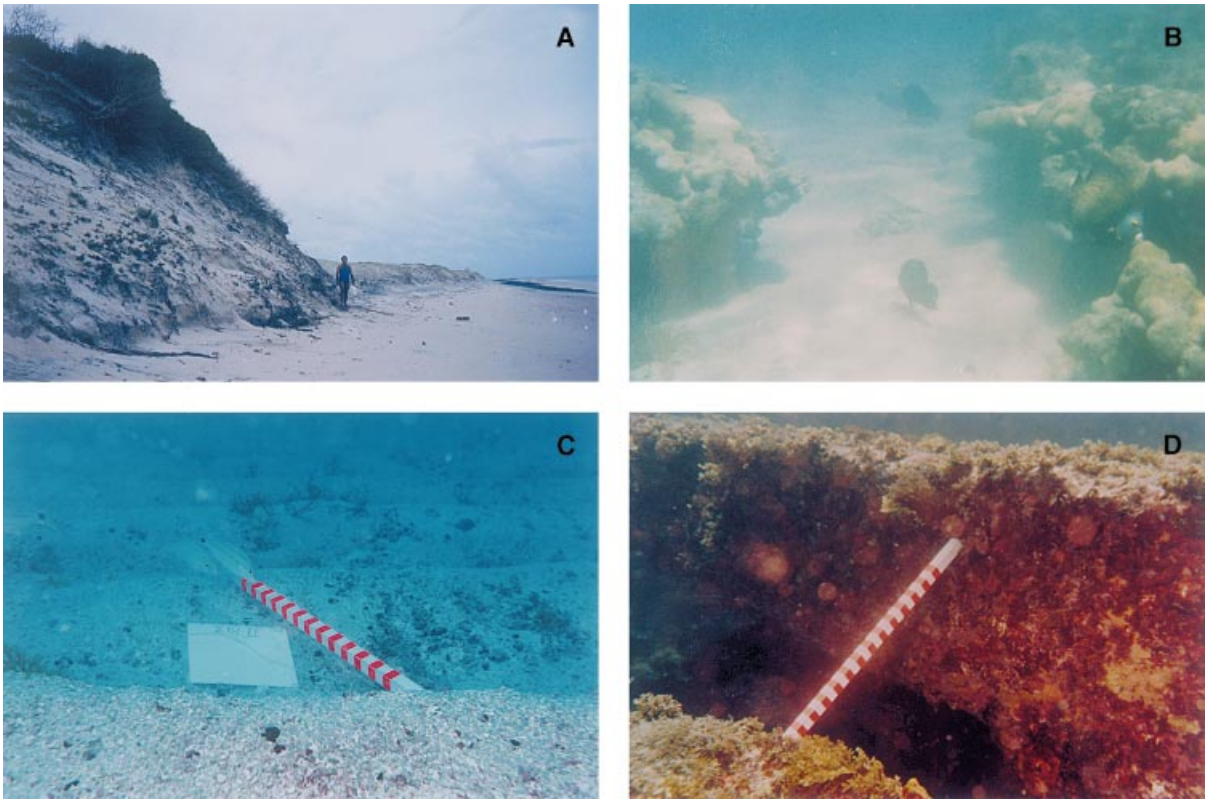

Fig. 3. Characteristic features of the sedimentary zones of the shallow shelf. (A) Coastal zone: siliciclastic sand beaches backed by subaerial dunes; (B) sublittoral turbid zone (2–10 m water depth): development of coral patch reefs (1 m in height), surrounded by medium-grained carbonate sand; (C) sand ribbon zone (10–18 m water depth): sand ribbon crest with superposed wave ripples developed in bioclastic gravelly sand with pink-coloured live branching coralline algae (scale in 2-cm intervals); (D) lithified sediment zone: carbonate-cemented sandstone forming seafloor rock outcrop. Note dense encrusting biota on sandstone (scale in 2-cm intervals).

ripples have also been observed but were not studied in detail. They are thought to be generated by short-term variations of shallow water waves and tidal currents. Offshore from the reefs are areas of coralline algae and *Halimeda*-rich sands with abraded and reworked beds of rhodoliths that are generally colonized by fleshy brown or red algae.

Sand ribbon zone (SRZ)

This 8- to 10-km-wide zone lies seaward of the STZ and down to depths of 20 m. It comprises a field of longitudinal sand patches (south-east) and sand ribbons (north-west) aligned parallel to the coastline. These structures are visible on the Landsat image as subparallel, lighter and darker stripes, which correspond to crests and troughs of sand ribbons respectively (Figs 1, 2 and 3C). Sand streams appear as light areas, and their sediments are bioclastic carbonates; their surface is reworked to form large wave ripples. These grade into the lateral dark patches, which comprise stabilized algal beds, mainly composed of free-living coralline algae.

Subaqueous dune zone (SDZ)

This is a wedge-shaped area 1–10 km wide and at least 30 km long parallel to the coast. It passes to the south-east into the algal stabilized zone (ASZ) and to the north into the lithified sediment zone (LSZ) (Fig. 2). This zone comprises a featureless sand plain in its south-eastern (upstream) apex and a field of very large, asymmetrical, transverse dunes travelling downstream to the north-west. The bedforms are superposed by large wave ripples and are composed of quartz sands with less than 5% carbonate grains (*Halimeda* plates and small mollusc shells). The troughs of the very large dunes consist either of dead rhodolith beds associated with dense seaweed or of living coralline algal maërl (beds of free-living branching coralline algae).

Table 2. Nature and occurrence of bedforms on the Rio Grande do Norte inner shelf, NE Brazil. Mean grain size was estimated based on Folk & Ward (1957) and it is given in phi units, following Friedman & Sander's classification (see McManus, 1988)

DATE	SITE NUM.	LOCATION Lati. Long.	DEPTH (m)	BEDFORM TYPE	ORIENTATION TO COAST	ORIENTATION (average)	HEIGHT (cm)	SPACING (cm)	SEDIMENTS point count (n=400)	MEAN GRAIN SIZE	TEXTURE
SUBLITTORAL TURBID ZONE											
17/2/94	115	05°14'09 S 035°22'21 W	6.5	Mound(?)* ripple **	Parallel to the coast * 270° **	0° * 270° **	100 * ?	? ?	*Halimeda* Calcium carbonate: 98 %	M. sand 2.7	Sand
4/4/92	101	05°16'14 S 035°20'55 W	?	Large ripple	Parallel	?	15	75	Coralline algae and *Halimeda* Calcium carbonate: 100 %	F. gravel -0.87	Gravely-sand
31/1/94	501	05°15'44 S 035°21'08 W	5.4	Small ripple	Parallel	175°	4 - 5	38 - 50	*Halimeda* and coralline algae Calcium carbonate: 98.75 %	C. sand 1.5	Gravely-sand
31/1/94	502	05°15'23 S 035°20'08 W	5.6	Small ripple	Parallel, asymmetrical	175° (orient.) 260° (direction)	6	20	Coralline algae and articulated red algae Calcium carbonate: 96.5 %	C. sand 1.5	Sand
5/4/92	200	05°12'26 S 035°20'07 W	14	Large ripple	Parallel	NW -SE	11 - 12	70 - 75	Coralline algae, articulated red algae and molluscs Calcium carbonate: 96.5 %	V. c. sand 0.87	Sand
SAND RIBBON ZONE											
31/1/94	507	05°13'45 S 035°15'56 W	13.1	Large ripple	Parallel	150°	13	80	Bioclastic sandy-gravel, mainly coralline algae Calcium carbonate: 97.13 %	V. c. sand 0	Sandy-gravel
26/3/92	305	05°09'23 S 035°21'44 W	14.5	Large ripple	Parallel	165	11	70	Coralline red algae, articulated red algae, *Halimeda*. Calcium carbonate: 94.5 %	V. c. sand 0.97	
31/1/94	506	05°14'00 S 035°16'27 W	11.6	Small ripple	Parallel	170°	8	48	Coralline algae and articulate coralline Calcium carbonate: 95.38 %	V. c. sand 0	Gravely-sand
7/2/94	509	05°12'02 S 035°13'55 W	14.8	Large ripple	Parallel	147.5°	18	100 - 150	Bioclastic sandy gravel, mainly coralline algae and *Halimeda* Calcium carbonate: 14.75 %	Small gravel -1	Sandy-gravel
8/4/92	406	05°04'48 S 035°24'18 W	15.4	Small ripple	Parallel	NW-SE	4 - 6	60	Siliciclastic, *Halimeda* and coralline algae Calcium carbonate: 25 %	V. c. sand 0.67	Sand
24/1/94	406	05°04'50 S 035°24'18 W	14.4	Large ripple	Parallel, symmetrical and discontinuous, eventually crossing over each other.	145°	16	100	Siliciclastic, coralline algae and *Halimeda* Calcium carbonate: 50.75 %	C. sand 1.2	Sand
7/4/92	310	05°06'50 S 035°19'37 W	15.9	Small ripple	Parallel		8	50	Coralline algae, *Halimeda* and siliciclastic Calcium carbonate: 96.5 %	V. c. sand 0.03	Gravely-sand
26/3/92	311	05°06'20 S 035°19'12 W	17.0	Small ripple	Parallel	170	8	40	Coralline algae, *Halimeda* and siliciclastic Calcium carbonate: 94.5 %	V. c. sand 0.67	Sand
8/4/92	408	05°04'03 S 035°23'45 W	15.4	Small ripple	Parallel	NW-SE	12 - 13	50	Coralline algae, *Halimeda* and siliciclastic Calcium carbonate: 84.75 %	C. sand 1.2	Gravely-sand

24/1/94	408	05°04'00 S 035°23'44 W	16.7	Large ripple	Parallel, symmetrical with sharp top symmetrical rounded top	138°	20 16	20 - 150 72	Coralline algae, *Halimeda* and siliciclastics Calcium carbonate: 81.25 %	V. c. sand 0.63	Gravely-sand
4/4/92	110	05°15'13 S 035°11'40 W	16.9	Small ripple	Parallel	NE-SW ?	4	45	Coralline algae and *Halimeda* Calcium carbonate: 98 %	F. gravel -0.77	Gravely-sand
23/1/94	218-2	05°09'11 S 035°15'58 W	16.7	Large ripple	Parallel, symmetrical truncated by seaweed growth	152°	15 25	- 70-1 m	Siliciclastic, coralline Calcium carbonate: 44 %	V. c. sand 0.1	Gravely-sand
23/1/94	218-1	05°09'07 S 035°15'48 W	15.4	Large ripple	Parallel, symmetrical to asymmetrical	148°	18	90	Coralline and siliciclastics Calcium carbonate: 40 %	?	Sand
23/1/94	218	05°08'57 S 035°15'49 W	16.5	Large ripple	Parallel, symmetrical	137.5°	25	112	Coralline algae, siliciclastics and *Halimeda* Calcium carbonate: 77.5 %	F. gravel -0.07	Gravely-sand
5/4/92	218	05°08'58 S 035°15'47 W	15.7	Large ripple	Parallel	NW -SE	14	85	Coralline algae siliciclastic and *Halimeda* Calcium carbonate: 77.5 %	V. c. sand 0.37	Sand
23/1/94	314-1	05°05'51 S 035°18'49 W	14.1	Large ripple	Chaotic, symmetrical asymmetrical	137.5°	20 4 - 6	90 60	Coralline algae, siliciclastic and *Halimeda* Calcium carbonate: 70.5 %	V. c. sand 1.5	Sandy-gravel
SUBAQUEOUS DUNE ZONE											
2/4/92	317	05°04'04 S 035°17'16 W	18.7	Small ripple	Parallel * transverse**	120° 300°	2 * 2*	40* 15**	Siliciclastic Calcium carbonate: 4 %	C. sand 1.5	Sand
9/4/92	A400	05°01'05 S 035°22'46 W	20.0	Small ripple	Parallel	?	8	45	Siliciclastic Calcium carbonate: 31 %	C. sand 1.6	Sand
21/1/94	803-1	05°04'04 S 035°18'59 W	13.7-20.7	Very large dune	Transverse, asymmetrical	60°	700	5000	Siliciclastic sand, minor bioclasts . Calcium carbonate: <15 %		Sand
			13.7 20.7	Small ripple	Parallel	120°	14	70	Siliciclastic sand Calcium carbonate: 5.75 %	M. sand 2.4	Sand
			20.7	Ripple	Parallel	120°	4	14	Siliciclastic sand	M. sand 2.6	Sand
			20.7	Large ripple	Parallel	120°	10	65	Siliciclastic and coralline algae	C. sand	
				Large ripple	Parallel	120°	12	70	Bioclastics-corallines, bryozoans Calcium carbonate: 25 %	C. sand	Gravely-sand
21/1/94	803-2	05°03'29 S 035°19'57 W	16.1	Large ripple	Parallel, symmetrical (top of v.l. dune)	135°	18	96	Siliciclastic sand with minor contribution of bioclasts Calcium carbonate: 14.75 %	C. sand 1.5	Sand
LITHIFIED SEDIMENTS ZONE											
9/4/92	418	05°58'25 S 035°20'49 W	16.7	Small ripple	Parallel	NW-SE	10 - 12	55-60	Siliciclastic Calcium carbonate: 3.25 %	C. sand 1.37	Sand
18/2/94	326	05°03'07 S 035°16'02 W	18.0	Small ripple	Parallel, symmetrical		5	37	Coralline algae, *Halimeda* and molluscs Calcium carbonate: 84 %	C. sand 0.7	Sandy-gravel

Algal stabilized zone (ASZ)

This Y-shaped zone (Fig. 2) is situated seawards of the SRZ and partially encloses the SDZ to the north-west (Fig. 1). It consists of free-living coralline algal maërl that has been stabilized by the intergrowth of their branches. It is often populated by starfish and has a variable cover of fleshy benthic algae. Seaweeds such as *Valonia macrophysa* and *Halimeda gracilis* were also observed to contribute to the stabilization of the coralline algal beds in sites of production.

Lithified sediment zone (LSZ)

This zone is oriented NW–SE and forms the margin of the inner shelf area (Figs 1 and 2). It has a maximum width of 4 km and is approximately 50 km long within the study area. It comprises underwater rocky outcrops with heights of 0·3–4·0 m above the sea floor (Fig. 3D). The carbonate grains (foraminifera, molluscs and calcareous algae), structures (plain bedding) and fabrics of these rocks indicate that they are of shallow marine origin. There are two main lithologies: carbonate-cemented sandstones, more or less rich in bioclasts, and bioclastic grainstones–packstones (with ^{14}C dates of 6000–31 000 years BP; Testa, 1996; Testa *et al.*, 1997).

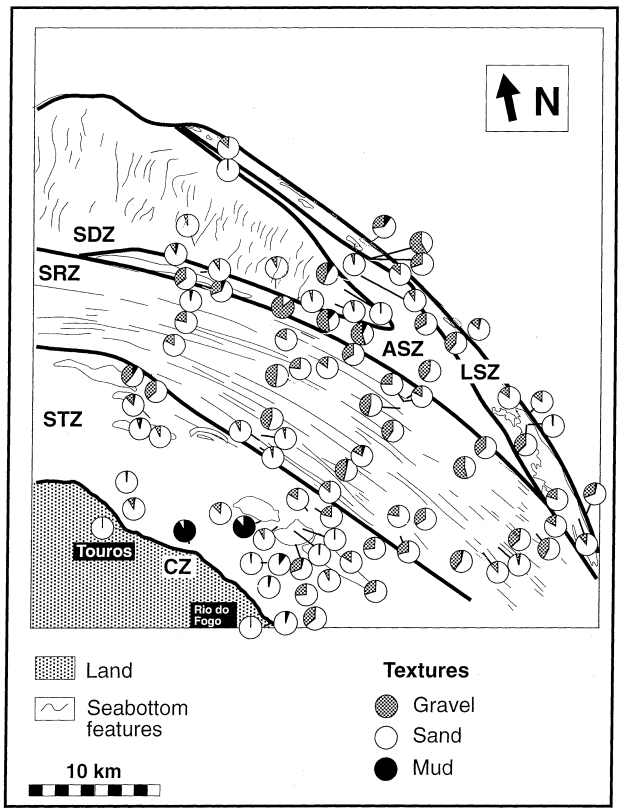

Fig. 4. Pie diagrams illustrating the relative percentages of mud, sand and gravel within different sediment zones.

SURFACE SEDIMENT CHARACTERISTICS AND TRANSPORT DIRECTIONS

Surface sediment texture and composition

The surface sediments are characterized by carbonate and siliciclastic sands and gravels mostly depleted in mud (Fig. 4). Fine- to coarse-grained sands dominate in the nearshore areas, and sands increase in grain size from medium to coarse grained in the vicinity of the patch reefs. The westerly (protected) side of the patch reefs and the partially exposed nearshore rocks provide sheltered areas where the only accumulations of muddy sediments are found. These sediments appear in serial Landsat TM images as plumes of suspended sediments moving off the reef area. There is little evidence of mud derived from river input. The sediments gradually coarsen offshore from the coral patch reefs and vary from coarse- to very coarse-grained sands and gravelly sands in the area of the sand ribbons (Fig. 4). Sediments are generally unimodal passing to bimodal distributions adjacent to sites of carbonate production offshore. Sediments range from gravelly sands and very coarse to medium sands in the south-east (SRZ and ASZ) to medium- to fine-grained sands in the north-west (SDZ) part of the study area (Fig. 4).

The area has well-defined areas of carbonate and siliciclastic deposits (Fig. 5). Sediments dominated by siliciclastics (<50% carbonates) are found in the CZ and in much of the SDZ. Mixed carbonate–siliciclastic sediments are found in the nearshore area between the CZ and STZ. They also occur towards the borders of the SDZ and in the inshore side of the LSZ. The carbonate-dominated areas (>50% carbonate) are most of the STZ, the entire SRZ and ASZ, and the outer portions of the LSZ.

Point counting reveals that the carbonate sediments are dominated by calcareous algae (> 80% coralline red algae, *Halimeda* and articulated coralline algae) in both nearshore and offshore regions (Fig. 6). There is a strong correlation ($r = 0{\cdot}75$) between the main carbonate contributor, coralline red algae, and the bulk carbonate content (Fig. 6), indicating that

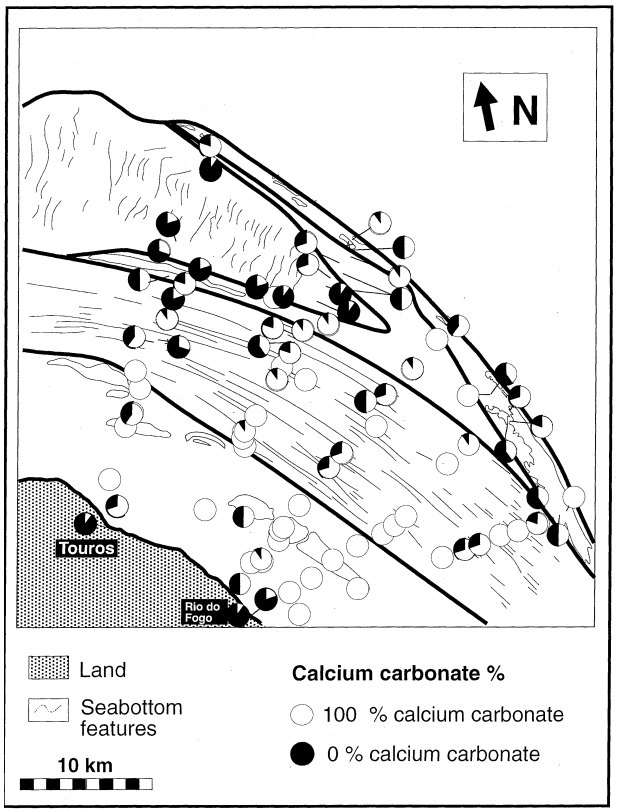

Fig. 5. Pie diagrams representing the carbonate–siliciclastic percentages of sediments (based on point counting) at the sites investigated. Note siliciclastic-rich areas in coastal zone and offshore lithified sediment zone and subaqueous dune zone.

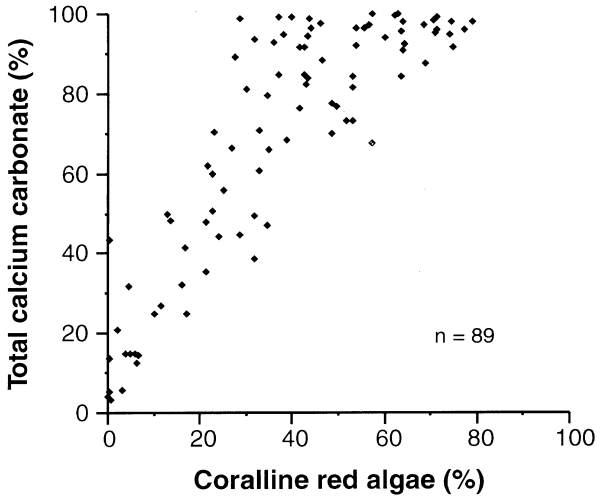

Fig. 6. Relationship between the percentage of coralline algal grains and the total carbonate percentage obtained from point counting.

corallines are the principal carbonate grain producers over the entire range of sediments. The siliciclastic component is mainly composed of medium to fine quartz sands with a local contribution of quartzose pebbles at some sites in the middle of the SRZ and in the LSZ.

BEDFORMS OF THE SAND RIBBON ZONE (SRZ)

The SRZ has two distinct suites of bedforms: the large-scale sand ribbons as seen in the Landsat image (Fig. 1), and the small-scale bedforms sampled and measured in the field.

Sand ribbons

Description

Sand ribbons (*sensu* Kenyon, 1970) occur in the middle portion of the study area, in water depths of 7–17 m, lying parallel to the coast and offshore to the patch reefs of the sublittoral turbid zone (STZ). The axes of the ribbons curve from a NW–SE to a WNW–ESE orientation in a downstream NW direction (Fig. 7). The length of individual sand ribbons varies between 2 and 12 km, and they vary between 180 m to 580 m in width. Diving investigations (stations 218, 218-1, 218-2 and 314, 314-1, 314-2; Fig. 8) show that the ribbons are very low relief structures with heights of just 1–3·5 m.

The crests of the sand ribbons are composed of coarse, white, bioclastic carbonate sands passing to gravelly sands towards the troughs (Figs 3 and 8), which are composed mainly of coralline red algal fragments (up to 70%) and *Halimeda* plates and fragments (up to 20%). The troughs are also characterized by dead rhodoliths, probably because of temporary burial. These vary in size, with intermediate axes between 3 and 6 cm and shapes varying between densely branched spherical (form IV; Bosence, 1983) to ellipsoidal and abraded forms. The sandy crests of the ribbons have poorly developed benthic communities; seaweeds are rarely found, with the exception of the green alga *Caulerpa prolifera*. This may be abundant enough to disrupt the small-scale bedforms (see below) and promote sand accumulations up to 50 cm in height above the surrounding sea floor. Other seaweeds occur if rhodoliths, generally dead, occur in the same area providing a hard surface for colonization. Agglutinated

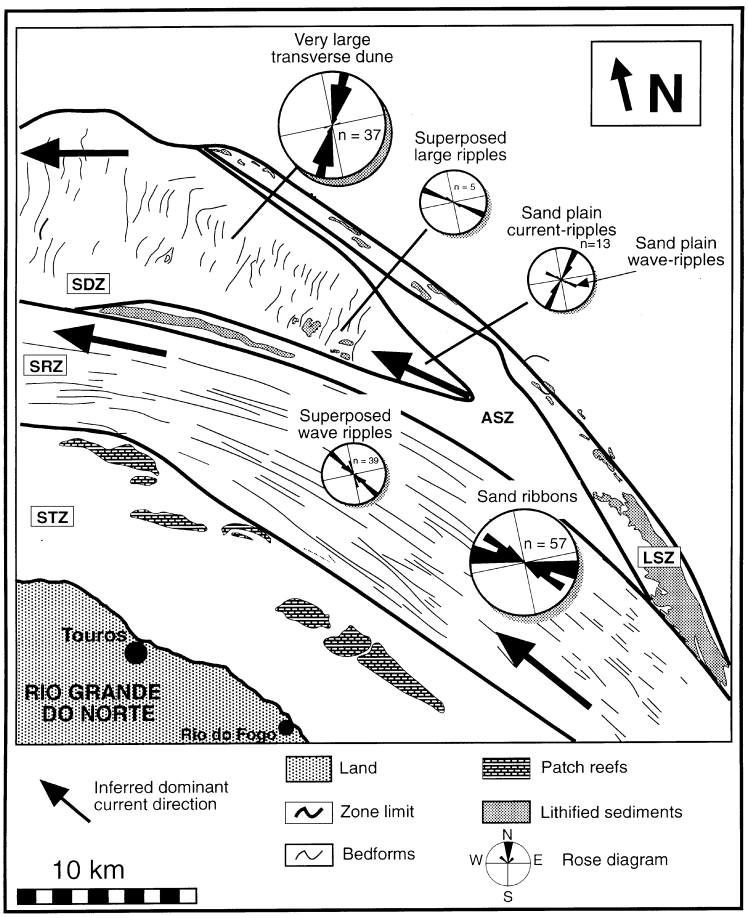

Fig. 7. Rose diagrams showing the crest orientations of large-scale bedforms and of small-scale bedforms and the inferred swing in regional current flow from NW to WNW. Note the orientation of the wave-generated, small-scale bedforms (ripples) normal to the large-scale structures.

polychaete tubes, up to 15 mm diameter, are also found protruding a few centimetres above the sediment surface, and reworked tubes are also found nearby, indicating sediment erosion. Siliciclastic pebbles are found locally in the middle portion of the sand ribbon field.

The gravel floors between sand ribbons are up to 1000 m wide, comprising bioclastic sands or gravelly sands (between 40% and 96% calcium carbonate) composed of coralline algae, *Halimeda* fragments and other minor contributors, e.g. foraminifera, molluscs and echinoid spines. The sands are partially stabilized by irregular patches of living, branching rhodoliths, which are usually colonized by seaweeds, particularly *Dyctiopteris plagiogramma*. Rhodoliths provide the only substrate available for colonization in these sites. The rhodoliths and epiphytes are observed to roll or saltate to and fro across the wave ripple crests in response to fair weather, oscillatory wave currents.

Rhodoliths and branching coralline maërl can also form belts perpendicular to the sand ribbons (Fig. 9) and the small-scale bedforms. These rhodoliths are not colonized so abundantly by seaweeds.

Sand patches (Belderson *et al.*, 1982) are interpreted from the Landsat images as the dominant features found south-east of the sand ribbons, where higher stabilization of the sea bottom by calcareous algae communities may occur.

Interpretation

Sand ribbons are a common feature in the English Channel (Kenyon, 1970; Belderson *et al.*, 1982; 1988; Kuijpers *et al.*, 1993), where they develop from flow-parallel, helical vortices with near-bed velocities of 100–140 cm s^{-1}. The mechanism of sediment transport is directed away from the coarse-grained sediment area and towards the sand stripes or crests (Allen, 1968; McLean, 1981), which is also interpreted to be the case in the study area. In three-dimensional flows, the disturbance of the flow is transverse to the motion, whereas the bedforms (sand ribbons) are oriented parallel to the flow. The cause of the flow instability is related to differential roughness and secondary flow near the bed between the coarse-grained trough and the finer grained crest (Allen, 1968; McLean, 1981; Pantin *et al.*, 1981). In

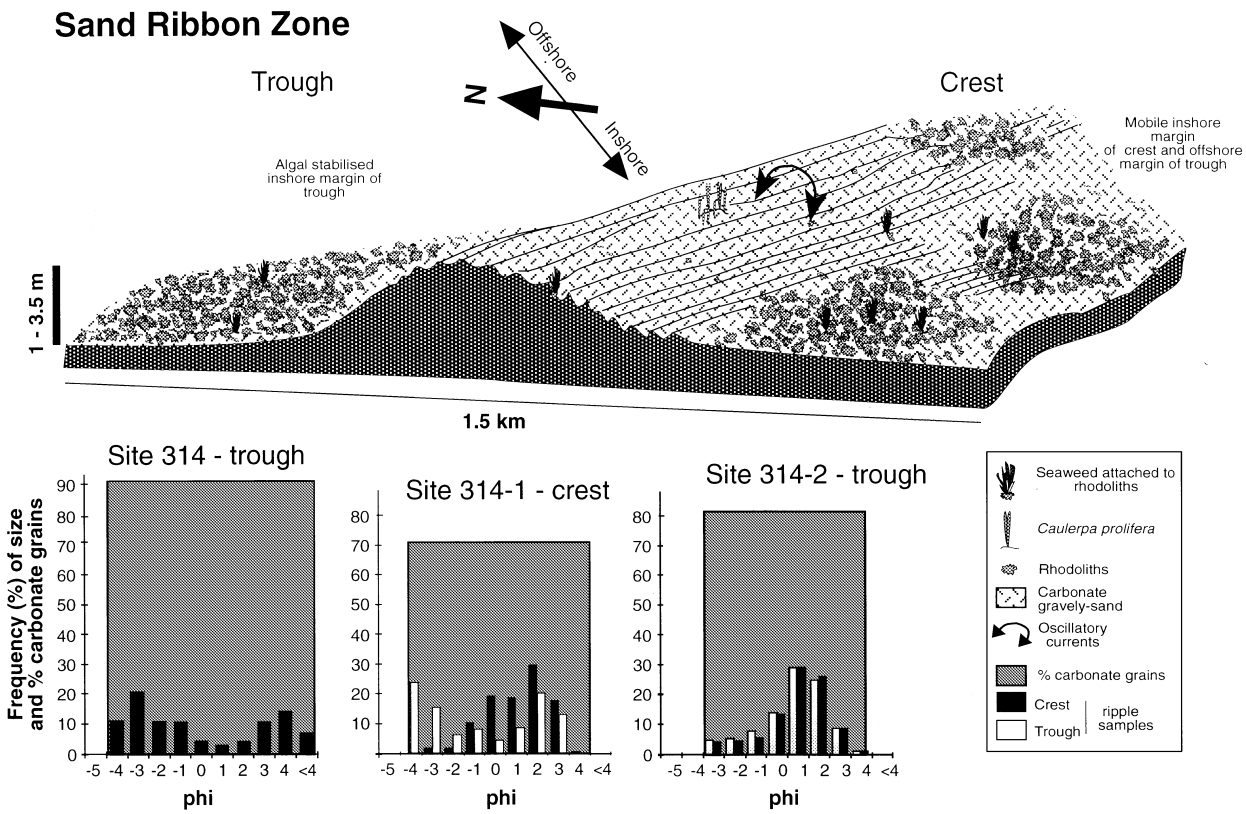

Fig. 8. Schematic diagram based on diving observations made along a transect across a sand ribbon. Textural and compositional analyses of samples collected during dives. Note that sediments are generally bimodal in both small and large bedforms.

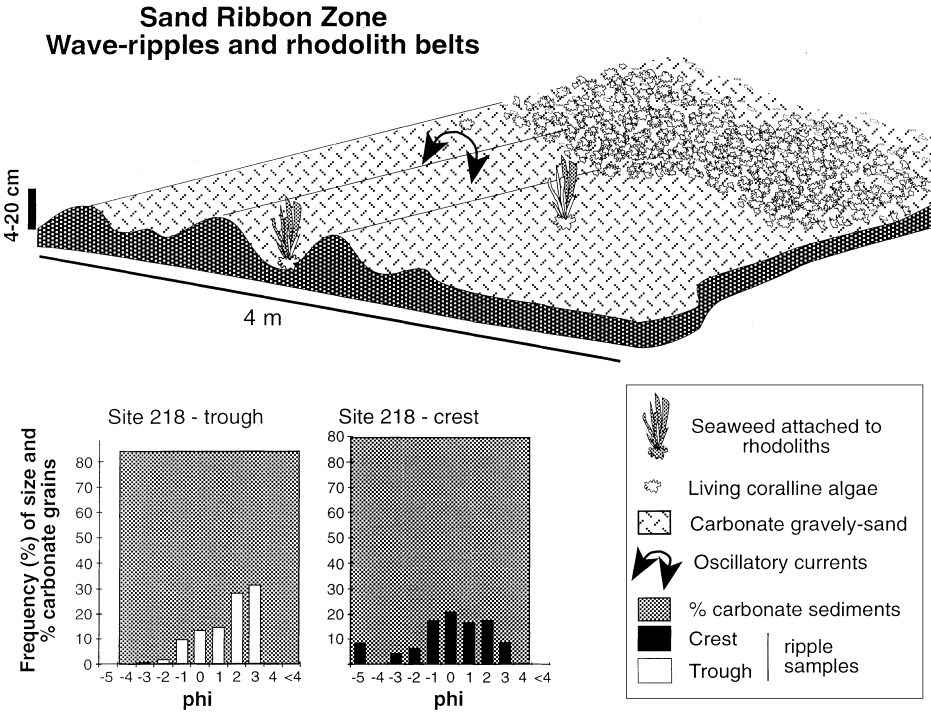

Fig. 9. Schematic diagram of branching rhodolith belt development perpendicular to the wave ripples and normal to the main flow direction. Rhodoliths may be found saltating to and fro across the crest of the wave ripples.

addition, interactions between currents and waves may also play a role in flow instability (Pantin, 1991). These bedforms are better developed in sediment-starved areas and on hard bottoms (Allen, 1968; Stride, 1970; Werner & Newton, 1975; McLean, 1981; Wilson, 1988). Recent work by Colombini (1993) showed that the simple occurrence of a coarse-grained and erodible bed is sufficient to develop a flow instability, without the need for lateral walls (see also Flood, 1983). The origin of the longitudinal bedforms in the study area may conform to the model proposed by Colombini (1993), whereas the maintenance of such structures seems to be in accordance with McLean's (1981) theoretical model for the dynamics of secondary, streamwise helical flow. The latter has been documented from *in situ* measurements in large water bodies by Wiekman *et al.* (1989). To the south-east of the study area, the ribbons are less continuous, being feather edged and resembling longitudinal sand patches (Fig. 1). Belderson *et al.* (1982) noted that these two varieties of bedforms have a similar origin and may grade from one into another. In the English Channel, the formation of such patches is associated with tidal currents of about 80 cm s^{-1} maximum; thus, they are slightly lower energy structures than sand ribbons. The downstream change in orientation of the large bedforms from NW–SE to WNW–ESE parallel to the coast line (Fig. 7) provides the main evidence that the bedforms are maintained by coast parallel unidirectional currents that are likely to be a combination of the North Brazil current (Stramma *et al.*, 1990), tidal currents (Mabessone & Coutinho, 1970) and wind-driven currents (da Silveira *et al.*, 1994). When combined, these coast-parallel currents are of sufficient strength during peak tidal flow conditions to generate sand patches in the south-east of the area and stronger currents in the central and north-western part of the area where sand ribbons are developed.

Bedforms superposed on sand ribbons

Description

Small and large wave ripples occur in bioclastic sands at the crest and on the flanks of the sand ribbons. They are generally symmetrical, with their crests having the same orientation as the underlying sand ribbon (Fig. 7). The small wave ripples are oriented NW–SE and have spacing varying between 37 cm and 60 cm and heights from 4 cm to 13 cm (Table 2, Fig. 7).

Large wave ripples are spaced at 70 cm and 150 cm with heights varying from 16 cm to 25 cm. Sharp and rounded crested bedforms may co-occur, and both morphologies are seen in the coarse coralline algal- and *Halimeda*-rich sands (40–96% $CaCO_3$). The sharp-crested ripples generally have a larger spacing and height compared with the round-crested bedforms. Small rhodoliths are commonly found at the crest of the bedforms, suggesting their active transport. Asymmetrical, large wave ripples with their lee side directed towards the coast were also found (Table 2, site 406). These are rich in siliciclastic pebbles, which accumulate preferentially in the slope and trough of the bedforms. These small bedforms may co-occur in two ways: small wave ripples superposed on large wave ripples; or large wave ripples with sharp-crested small wave ripples in their troughs, with parallel orientation.

Interpretation

The symmetrical morphology of these bedforms indicates that they are wave-formed structures, and this is confirmed from diving observations of oscillatory currents and grain entrainment (including rhodoliths <4 cm in diameter). Wave-generated carbonate bedforms with comparable dimensions and coarse-grained algal composition have been described from temperate carbonate environments (e.g. Bosence, 1976a; Farrow *et al.*, 1979; Terhorst, 1988).

The SE–NW orientation of the dune crests indicates that wave approach is oblique or perpendicular to the coast. The fact that these wave-generated ripples are freshly formed on the large-scale sand ribbons, which clearly relate to a different flow system, suggests that sediment movement of the larger scale structures is intermittent. Two explanations for this are proposed: either the large bedforms move annually in response to seasonally high currents in the austral winter (see above, *Environmental setting*); or they move much more frequently in response to periods of peak tidal flow, similar to the bedforms on the UK shelf (Belderson *et al.*, 1982). Diving could not be undertaken during either of these periods for safety reasons, but was undertaken soon after spring tides. The relative freshness of the large-scale bedforms and their generally meagre biota, as an indicator of frequent movement of sediments (cf. Wilson, 1982), leads us to favour the second hypothesis.

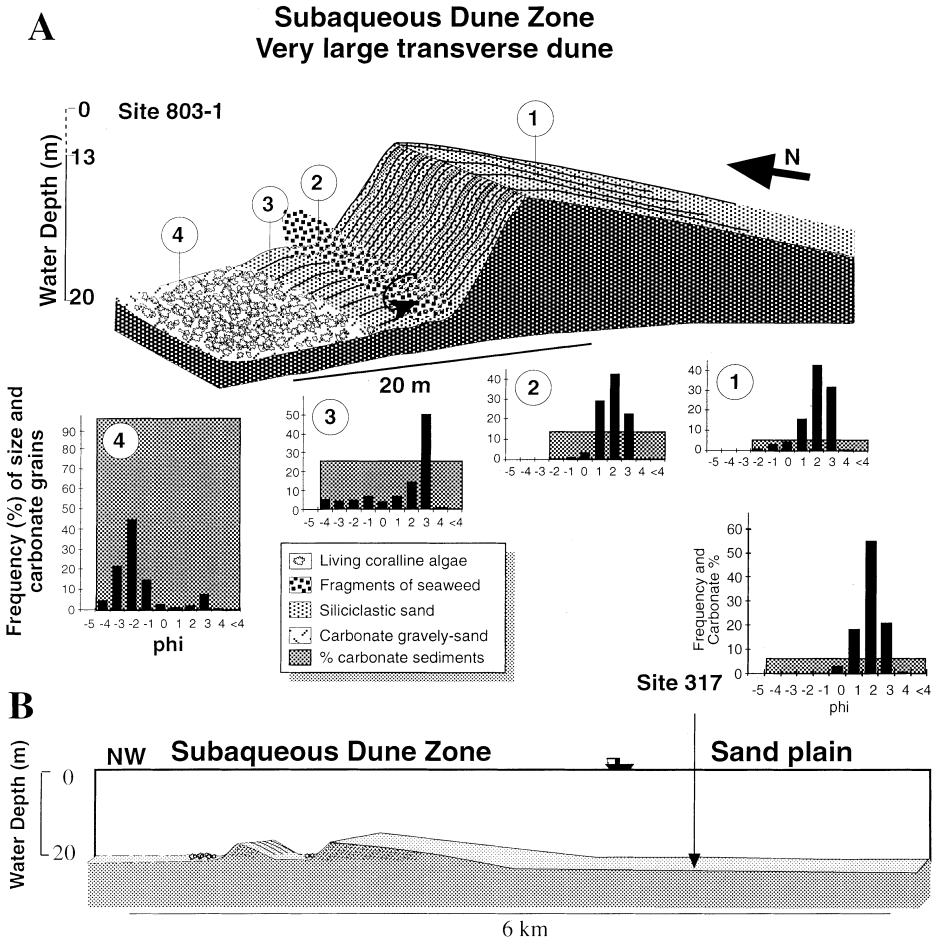

Fig. 10. (A**)** Schematic diagram of very large subaqueous dune within the SDZ. Note that the dune is superposed by large and small wave ripples, with crests aligned perpendicular to the very large dune. Samples of sediments collected during the dive show the gradual increase in grain size and percentage carbonate from dune crest to algal stabilized trough. (B**)** Schematic diagram of sand plain that occurs upstream of sand dune field. Wave and current ripples are found in this area developed in a quartz-rich sand. The area lacks carbonate-producing organisms, and no biogenic structures were seen in short cores.

Therefore, during fair weather and presumably also during storm conditions, the large-scale sand ribbons are modified by wave-generated oscillatory currents that provide a component of shoreward transport of rhodoliths and sediment.

BEDFORMS OF THE SUBAQUEOUS DUNE ZONE (SDZ)

The SDZ has three distinct suites of bedforms: very large transverse dunes, as seen in the Landsat image; and the smaller scale bedforms observed and measured in the field, which comprise superposed large wave ripples on very large transverse dunes and small wave ripples in the upstream sand plain (Fig. 7).

Very large transverse dunes

Description

These bedforms occur in the north-west portion of the SDZ and form a field of dunes of approximately 30 km down current and 10 km across (Vianna *et al.*, 1991) within the study area. This is downstream from a broad sand plain (Fig. 10A and B, Table 2). Two trains of dunes are found within the dune field: an inshore train with an average spacing of 840 m with dark (low reflectance from seaweeds) areas in between; and an outer train with more regular, but narrower, dune spacing (average 650 m). The orientation of the dune crests, measured from the Landsat TM image, varies between 280° and 307° in the inner train and between 180° and 314° in the outer train (Fig. 7), and varies from a NE–SW orientation in

the south-east to a NNE–SSW orientation downstream to the west. Dune crests measured from Landsat images vary between 1300 m and 5600 m in length, and dune heights vary between 3 m and 8 m (Vianna *et al.*, 1991).

While diving, the steep (around 30°) lee slopes were observed to consist of avalanching slip faces. This was also observed by Vianna *et al.* (1991) during a dive in the austral winter and provides clear evidence of active sediment transport during normal weather conditions.

The crests and foresets of the dunes are formed of well-sorted, fine- to medium-grained quartz sand. The small percentage (5%) of carbonate grains (molluscs, *Halimeda* and coralline algae) are coarser than the host siliciclastic sand, which suggests a hydraulic equivalence, as both are actively transported. The sediments at the base of the dune slope are composed of poorly sorted medium-grained quartz sands with an increased (<25%) calcium carbonate content (Fig. 10A). No living benthos was found on the tops and slopes of these dunes, suggesting that the sediments move frequently and also that carbonate sediments found in this setting are allochthonous, i.e. derived from neighbouring areas (cf. Wilson, 1982).

In contrast, the troughs are composed of coarse gravels, with carbonate percentages increasing to 100%, and are stabilized by living coralline algal maërl. The overall small sizes of the free-living coralline algae (−2 to −4 phi) and the low diversity of the benthos (mainly bryozoans) suggests that it is a young and possibly stressed community (cf. Wilson, 1979; 1986).

Seaweed fragments are entrained in vortices in the lee of the dune crest, which together with the sharp crest of the dunes, indicates that these bedforms are active and moving in a northwesterly direction. During periods of high flow separation, carbonates are entrained in the leeward vortex of the dune and are transported towards the dune slope rather than away from it. This pattern may partially explain the increase in calcium carbonate from the dune toe to the algal-stabilized beds, although much of the coarse carbonate here has been generated locally.

Interpretation

The very large subaqueous dunes found in the study area are similar to the transverse dunes that are common features of the shelves of north-west Europe (MacCave, 1971; Belderson *et al.*, 1982) and South Africa (Flemming, 1978; 1980). These

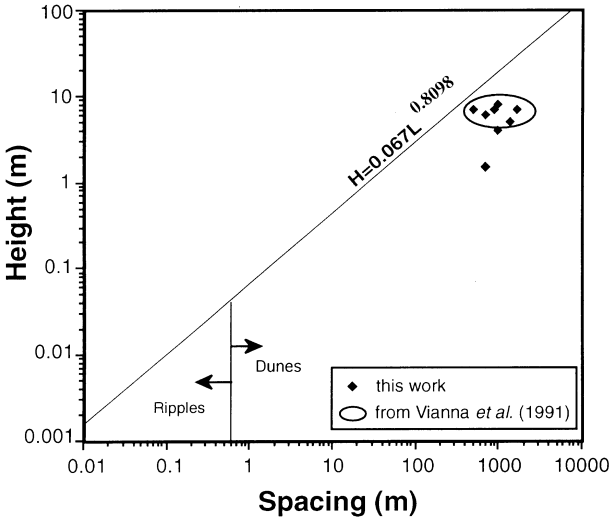

Fig. 11. Log-log plot of height vs. spacing of bedforms measured in this study, from a depth profiling by Vianna *et al.* (1991). Diagonal line gives height/space relationship of current-generated structures of Flemming (1988).

dunes are thought to be generated by two-dimensional flow with near-bed velocities between 60 and 75 cm s^{-1}. The change in orientation and spacing of the dunes from the inner to the outer dune trains suggests that the wide-spaced inner dunes are sediment starved and partially stabilized by the intervening algal-rich sea-floors, whereas the more narrowly spaced outer dunes are not so stabilized and may be moving faster than the inner dune train.

The relatively rapid transport of the siliciclastic dune compared with the more stable carbonate-rich troughs results in an enrichment of bioclastic material at the toe of the dune and is expected to produce a coarse, carbonate-rich layer underlying the dunes. The intermixing at the base of the preserved cross-stratification should provide evidence in ancient examples that these facies coexist and represent simultaneous accumulation of carbonate and siliciclastic grains.

It is generally accepted that the height of bedforms has a definite relationship with spacing, so an increase in spacing is accompanied by an increase in the volume and size of the bedform (Allen, 1968). From plots of spacing and height of over a thousand current-generated bedforms, Flemming (1988) suggested that the mean relationship between spacing (L) and height (H) is given by the relationship $H = 0{\cdot}067L^{0{\cdot}8098}$ (Fig. 11) for clastic bedforms.

Logarithmic plots of height and spacing for the large-scale, current-generated bedforms in this study area together with those published in

Vianna *et al.* (1991) are plotted in Fig. 11 (Table 2). This plot indicates that the height of the Brazilian bedforms is relatively low for their spacing, suggesting that these dunes are sediment starved (see Flemming, 1980; Figs 11, 13 and 14). Sediment starvation of these dunes has been attributed to a reduction in modern siliciclastic sources and supply of sediments, and also to the continuous carbonate production and seabed stabilization (see also general discussion).

Bedforms superposed on very large transverse dunes

Description

These bedforms comprise two-dimensional and symmetrical, large wave ripples in the stoss side and near the toe of the leeward side of the very large dunes and small wave ripples on their lee slope (Fig. 10A, Table 2). The orientation of the crests of the superposed bedforms, 120° NW–SE, is perpendicular to the crests of the very large transverse dunes (NE–SW to NNE–SSW) (Figs 7 and 10B). The large wave ripples have spacings of 0·65–0·7 cm and heights of 10–14 cm, whereas the small wave ripples measured on the lee slope have a constant spacing of 14 cm and height of 4 cm from the crest down to the toe of the dunes. The sediments comprise medium- to coarse-grained, well-sorted sand on the lee slope, medium- to very coarse-grained, moderately sorted sand in the toe of the slope and poorly sorted, medium-grained sand in ripples in the leeward trough (Fig. 10B).

Interpretation

These freshly formed superposed wave ripples with crests normal to the large-scale dunes indicate formation by a different mechanism. Their symmetry indicates that they are generated by oscillatory wave currents, possibly superimposed on tidal flow. The occurrence of the superposed structures indicates that unidirectional northwesterly and westerly sediment movement on the dunes is intermittent. Similar superposed wave-generated structures are described in the previous section on sand ribbons, and active transport of the ribbons and the dunes is expected to occur with peak tidal flow rather than seasonally. Onshore sediment transport by wave-generated currents is indicated by the occurrence and morphology of the ripples on the dunes.

Ripples on the sand plain area

Description

Transverse ripples are found in the sand plain, upcurrent from the very large transverse dunes (Figs 7 and 10B; Table 2). These bedforms are of two types: symmetrical wave ripples (45 cm spacing, approximately 300° crest orientation) and slightly asymmetrical ripples (15 cm spacing) transverse to the main flow (approximately 124° crest orientation) (Fig. 7). Both types are around 2 cm in height. The sediments consist of medium- to fine-grained siliciclastic sands with less than 5% calcium carbonate. This area has no obvious development of macrobenthos or burrows; short cores show no sedimentary structures or preserved burrows. Very small fragments of seaweed have been seen being transported into the area by currents, and these may be incorporated into the sediments.

Interpretation

The larger symmetrical bedforms are considered to be wave generated and of similar origin to the wave-formed superposed structures from the nearby transverse dune field. The smaller asymmetrical structures are considered to result from an overprint by occasional longshore currents reworking the sands. The absence of large-scale bedforms in this area is believed to result from the lack of sediment supply downcurrent from the ASZ.

DISCUSSION

Hydrodynamic controls on the occurrence of large-scale bedforms

The occurrence of the large-scale bedforms on this shelf is a simple pattern of inshore sand ribbons and offshore transverse large dunes. The sand ribbons occur in shallower waters (7–17 m) than the dunes (18–20 m water depth), and a higher hydrodynamic energy might therefore be expected. The occurrence of these marine shelf bedforms has been related to high peak tidal or ocean currents in the model developed by Kenyon (1970), Flemming (1980) and Belderson *et al.* (1982), whereby transverse dunes are replaced by sand ribbons with increasing flow rates. The application of the model of Belderson *et al.* (1982) to the Brazilian examples would be more unequivocal if there was a greater depth variation

between the two zones (SRZ and SDZ) on the Rio Grande do Norte shelf and if they had similar grain size and composition. However, there are major differences in grain size and composition between the two areas, and this may also have a bearing on the bedforms present. Although no experimental work has been carried out on the velocities required for entrainment of the sediments from this study area, it would be expected that the well-sorted medium-grained siliciclastic sands of the transverse dune zone would be eroded and transported at velocities of between 15 and 60 cm s^{-1} (Southard & Boguchwal, 1973).

Entrainment velocities for biogenic carbonate gravelly sands and coarse-grained sands are not so well known, mainly because of variations resulting from shape, size and density (Maiklem, 1968; Braithwaite, 1973; Steidtmann, 1982; Flemming, 1992). Prager *et al.* (1996) also suggest that bioclastic carbonates require a lower shear stress to initiate transport compared with siliciclastic grains. Grain density alone is a very variable parameter in bioclasts, and Jell & Maxwell (1965) found this to vary between 1·1 and 2·7 g cm^{-3}. However, experiments on fall velocity (Braithwaite, 1973) have shown that both medium-grained carbonate and siliciclastic grains have the same fall velocity of around 4 cm s^{-1}. Beyond this size, the fall velocities become distinct for each grain type, size and density, e.g. a 4·5-mm coralline algal grain has a similar fall velocity (21 cm s^{-1}) to a 2-mm quartz sand.

Coarse bioclasts such as rhodoliths often protrude well above the seabed, and rhodoliths have been observed to be transported easily by saltation in the field (see above). Bosence (1976b) recorded flume tank experiments in which rhodoliths may lift off directly from coarse beds into the flow, without significant rolling. The protrusion of coarse and irregular carbonate particles above the seabed thus decreases their threshold velocity, and movement is facilitated (Komar & Miller, 1973; Drake *et al.*, 1988; Prager *et al.*, 1996).

Therefore, the shallower water, coarser carbonate particles are expected to be as easy, or easier, to transport than the finer grained offshore quartz sand and, therefore, higher inshore velocities may not be necessary for the generation of the sand ribbons. In addition, the very coarse carbonate grains will increase bed roughness and contribute to flow instability and three-dimensional flow, which is required for sand ribbon formation. The fact that bioclastic sediments appear to have an extended lower plane bed transport phase than equivalent sized siliciclastic sands (Flemming, 1992) also supports the interpretation above.

Sediment production and supply

The origin and supply of siliciclastic and carbonate sediments within the study area is an unusual and important aspect of this shelf sedimentary system.

Siliciclastic sand supply

On a regional scale, siliciclastic sediments are concentrated in the coastal zone and in the more offshore subaqueous dune zone and lithified sediment zone (Figs 1 and 5). In the coastal zone, the quartz sands are swept along in a spectacular series of beaches and dunes (Mabesone & Coutinho, 1970; Cunha *et al.*, 1990). However, immediately offshore from this siliciclastic-dominated coast, biogenic carbonate sediments are being produced and are accumulating (Fig. 5). This indicates that the present-day, coastal siliciclastic sands are derived from reworked coastal sands by coast-parallel winds and currents (Fig. 7). This contrasts with many coastal dune belts where sands are derived from sublittoral sites by onshore winds/waves. The nearshore siliciclastic sediments are apparently being covered gradually by the constant sublittoral production of carbonate sediments and their transport into shallower waters. These shallow inshore areas are characterized by biogenic carbonate sands, gravels and occasional patch reefs.

The offshore area of the shelf has an isolated siliciclastic dune field. This is the reverse situation to many modern mixed clastic/carbonate shelves, which are dominated by siliciclastic sediments in the nearshore, but have carbonate-rich, clastic sediment-starved outer shelves (e.g. Emery, 1968; Flemming, 1978; 1980). These sands must be generated locally, because the dune field is isolated and bordered inshore by carbonate-rich sediments and offshore by a relatively steep slope with bioclastic muds to the outer shelf. As the sands are being transported to the north-west, they presumably must have originated some way to the south-east of the subaqueous dune zone. The most probable origin for these sands is through long-term reworking of sands from the lithified sediment zone, as these sandstones are composed of similarly mature, well-sorted, quartz-rich, medium- to coarse-grained sands. The origin of these sandstones is complex, and

it is possible that they represent either beachrocks formed during a late Pleistocene–early Holocene lowstand, which is indicated by bulk ^{14}C dates (6000–31 000 years BP; Testa *et al.*, 1997) and has been suggested previously by Vianna *et al.* (1993), or outcrops of earlier Quaternary shallow marine to continental deposits. The sandstones are today (and were presumably also in the past) undergoing erosion and bioerosion near the sea floor, which results in the erosion, undercutting and collapse of large blocks to the seabed (Testa, 1996a; Testa *et al.*, 1997). The erosion and supply of sand-sized material is limited today, because the outcrops are being encrusted by coralline algae, sponges and seaweed, which generate pockets of bioclastic sand and gravel locally. Inshore and downcurrent from these outcrops, there are, first, the stabilized algal zone, then the sand plain and transverse dunes of the SDZ. Thus, the only likely site for the supply of sand is from earlier erosion of these sandstones before the colonization of encrusters that essentially shut off the sand supply. Therefore, the dune field appears to have been isolated from its sand source, and this is reflected in the upstream sand plain and the widely spaced and sediment-starved dunes.

Carbonate sand supply

The sand ribbons are not only genetically distinct from the very large transverse dunes, but they are also different in that they are mostly composed of bioclastic carbonate sands and gravels. Field investigations show that skeletal carbonate, particularly from live stands of coralline algae, *Halimeda* and molluscs, are continually being supplied, transported and deposited within the region. Coralline algae are ubiquitous producers of carbonate gravel and sand (Fig. 6), and they dominate throughout the area. Molluscs are only abundant near sheltered areas. *Halimeda* is more patchy, being concentrated in the inshore areas of the SDZ (*H. incrassata*), in the ASZ (*H. gracilis*) and on the exposed surfaces of buried reefs. Disarticulated plates are transported inshore along with dead rhodoliths. The coral patch reefs do not significantly contribute sand-sized and gravel-sized material to the inner shelf. There is thus no locus of carbonate production within the region, and it appears, in contrast to the siliciclastic sand, to be produced more or less uniformly over the area of the inner shelf that has been investigated.

The factors controlling the occurrence of the large-scale, sublittoral bedforms are therefore not straightforward and, in addition to hydraulic energy, relate to sediment composition, which is, in turn, controlled by the historical development of the shelf and the interplay between widespread sublittoral biogenic carbonate production and two separate areas of siliciclastic sand supply.

Macrobenthic communities associated with large-scale bedforms

The bedforms within the entire study area are composed of variable amounts of siliciclastic grains, non-articulated and articulated coralline algae, *Halimeda* plates, mollusc shells and other minor contributors. These sediments are either autochthonous or transported from nearby sites of carbonate production or siliciclastic source areas. Large-scale bedforms are generally too mobile to sustain a diverse benthic community, and the rate of mobility and sediment transport of these bedforms may be assessed by the maturity or diversity of the biological community (cf. Holmes & Wilson, 1985; Wilson, 1986; 1988; Belderson *et al.*, 1988). Low-diversity, benthic communities are characteristic of very high-energy environments, in which sedimentation constantly disrupts the settlement and growth of benthic organisms (Wilson, 1986; 1988).

The crests of the sand ribbons and the dunes are similar in that they are composed of mobile sand with little or no benthos. However, the intervening troughs of both types of bedforms have more diverse biota and are the main production sites of calcareous algal sediments. The stage of development of these trough communities varies from what are interpreted as young communities dominated by coralline algal maërl, bryozoans and starfish to more diverse mature communities composed of coralline algal maërl, rhodoliths, seaweeds, *Halimeda*, starfish, bivalves, gastropods, sponges and octopus. These more mature communities are visible on the Landsat images as darker areas, whereas the young communities cannot be differentiated from mobile sediment.

The troughs of the sand ribbons are found to have both young communities and mature communities, depending on the position within the trough. During diving transects across sand ribbons and troughs, it was noticed that the inshore margins of the troughs have a more mature community developed compared with the offshore margins of the troughs (Fig. 8). If this

pattern is common to other sand ribbons, as is suggested by the occurrence of darker grey levels in these sites on Landsat images, then the inshore trough margins are more stable. The offshore trough margins and the adjacent inshore margins of the sand ribbons (Fig. 8) are subjected to more disturbance, resulting in younger communities. This is thought to relate to an element of onshore sediment transport, in the form of either small-scale, fair-weather, wave-driven currents or asymmetry in the vortices that generate the troughs and ribbons. The offshore portions of the troughs are thought to be disturbed, as they receive sediment from the adjacent sand ribbons, whereas the inshore margins would be more stable and permit the development of the more mature benthic community. This pattern of community stability suggests that there is an overall displacement of the sand ribbons towards shallower waters, where their development may be depth limited by erosional nearshore currents and waves or by the occurrence of obstacles such as patch reefs.

The troughs of the very large transverse dunes can be clearly seen to vary in grey scale in the Landsat image (Fig. 1). The mature (darker) communities occur only in the troughs of the inner train of dunes, and the offshore portion of the dune field has younger (lighter) trough communities. This suggests that the outer train of dunes is moving faster than the inner dune train and/or that the inner train is gradually being stabilized by algal colonization in the troughs. This may be the explanation for the change in orientation of the dune trains with the inner train with crests oriented NE–SW, while the crests of the outer dune train swing around to a NNE–SSW orientation (Fig. 7). Diving observations indicate that the lateral margins of the dunes may be more stabilized than the central portions. This leads to the central portion moving downcurrent with respect to the lateral margins and may explain the convex downstream curvature of many of the dune crests seen on the satellite images (Figs 1 and 7).

CONCLUSIONS

1 Based on Landsat image analysis ground-truthed by diving transects, the north-east Rio Grande do Norte shelf is redefined as a carbonate-rich shelf and divided into six sedimentary zones aligned parallel to the coastline and the inner shelf margin.

2 Detailed diving observations and sampling of the sand ribbon zone and subaqueous dune zone indicate that the occurrence of large-scale bedforms is the result of strong longshore oceanic and wind-driven currents. Similar processes are described from the eastern South African shelf (Flemming, 1980). Contrary to what is found on the South African shelf, the nearshore shallower areas develop sand ribbons, and deeper offshore areas develop very large transverse dunes. Previous models of large-scale, marine bedform generation (e.g. Belderson *et al.*, 1982) predict that the inshore, slightly shallow areas with sand ribbons would be swept by higher velocity currents. However, the small differences in depth between the two areas, the fact that the offshore areas are rich in quartz sand and that shallower areas are rich in coarse-grained gravelly carbonate sands, suggest that higher velocities may not be required to develop sand ribbons in inshore sediments. The larger, lower density, carbonate sediments, often protruding from the sea bed, require lower entrainment velocities and have a more extended lower plane bed transport phase than size-equivalent siliciclastic sand. Therefore, the formation of sand ribbons may have been triggered by the coarse, irregular, calcareous, algal growth, whereas their maintenance is directly related to the high hydrodynamic setting of the sand ribbons.

3 While the occurrence of large-scale bedforms is related to oceanic/wind-driven currents (alongshore transport), the superposed, small-scale bedforms are largely wave and tide generated in both fair and stormy weather conditions and result in shoreward-directed sediment transport.

4 The interdune and intersand ribbon troughs are stabilized to various degrees by free-living, branching, coralline algae and soft, macrobenthic algae together with benthic invertebrate communities. These become more diverse the longer the sea bed is stabilized and not affected by moving sediment. In the very large transverse dunes, the stabilization of the troughs of the dunes is thought to contribute to the stabilization and orientation of the dunes. In the sand ribbons, the difference in maturity of inter-ribbon trough communities indicates that sand ribbons have a shoreward component of movement as well as a downcurrent component.

5 The shelf is unusual in having two isolated sources of siliciclastic sand supply, which relate to the Quaternary flooding history of the shelf. A time-limited, offshore sand supply is found on

the outer part of the inner shelf, where former Quaternary shoreline sands have been eroded to form an isolated sand supply forming the present-day subaqueous dune field. The present-day coastal zone is formed by subaerial dunes and beaches of siliciclastic sands, which are recycled by longshore wind, wave and tidal currents. These sands are mostly isolated from the near-shore, shallow water carbonate sediments.

6 Carbonate sediment production occurs over much of the inner shelf zone and is dominated by calcareous algae with minor coral patch reefs. Coralline algae dominate and are produced in maërl beds, rhodoliths and encrusting corallines over lithified substrates. *Halimeda* is a common sand producer locally in both inshore and off-shore areas.

7 The continental shelf of north-east Brazil has a complex interplay of carbonate and siliciclastic facies. Today's carbonate sediments are gradually burying an earlier siliciclastic template. This gently shelving inner shelf area experiences extremely high hydrodynamic energy derived from the combination of oceanic, wind-driven, wave and tidal currents, resulting in large-scale marine bedforms within a shallow algal-dominated carbonate production zone.

ACKNOWLEDGEMENTS

This research has been undertaken with a CNPq grant (260178/91.8) to V. Testa, with fieldwork and radiocarbon dating funded by the Natural Environmental Research Council, UK (GR9/12660), and this financial support is gratefully acknowledged. We wish to acknowledge our thanks to Dr Marcio L. Vianna, Instituto Nacional de Pesquisas Espaciais, São José dos Campos, Brazil, for instigating the project, provision of Landsat images and logistical support. Professor Ayup-Zouain, Universidade Federal do Rio Grande do Sul kindly helped with our sampling strategy. Fieldwork in these remote and difficult seas could not have been undertaken without the dedicated help of Mr José Bezerra Neto, Mr Mário S. Testa, Dr Christine Perrin and the fishermen of Touros (Mr Oliveira) and Rio do Fogo. V.T. acknowledges encouragement and fruitful discussions during the Marine Studies Group Meeting, UK (Autumn 1994). We also thank John Wilson, Marcio Vianna, referees A. Coe, B. W. Flemming and D. M. Grammer, and editor Julian Andrews for their constructive criticism of our earlier manuscripts.

REFERENCES

Alexandersson, E.T. and Milliman, J.D. (1981) Intragranular Mg-calcite cement in *Halimeda* plates from the Brazilian continental shelf. *J. Sedim. Petrol.*, **51,** 1309–1314.

Allen, J.R.L. (1968) Some recent advances in the physics of sedimentation. *Proc. Geol. Assoc.*, **80,** 1–42.

Allen, J.R.L. (1985) *Principles of Physical Sedimentology.* George Allen & Unwin, London.

Andrade, G.O. (1964) *Os Climas.* In: *Brasil a terra e o homem. 1. As bases físicas* (Ed. by A. Azevedo), pp. 397–457. Companhia Editôra Nacional.

Ashley, G.M. (1990) Classification of large-scale subaqueous bedforms: a new look at an old problem. *J. Sedim. Petrol.*, **60,** 160–172.

Belderson, R.H., Johnson, M.A. and Kenyon, N.H. (1982) Bedforms. In: *Offshore Tidal Sands – Processes and Deposits* (Ed. by A. H. Stride), pp. 27–57. Chapman & Hall, London.

Belderson, R.H., Wilson, J.B. and Holme, N.A. (1988) Direct observation on longitudinal furrows in gravel and their transition with sand ribbons of strongly tidal seas. In: *Tide Influenced Sedimentary Environments and Facies* (Ed. by P. L. de Boer *et al.*), pp. 79–90. D. Reidel, Dordrecht.

Bosence, D.W.J. (1976a) *Ecological and sedimentological studies on some carbonate sediment producing organisms. Co. Galway, Ireland.* PhD thesis, University of Reading, UK.

Bosence, D.W.J. (1976b) Ecological studies on two unattached coralline algae from western Ireland. *Palaeontology*, **19,** 365–395.

Bosence, D.W.J. (1983) Description and classification of rhodoliths (rhodoids, rhodolites). In: *Coated Grains* (Ed. by T. M. Peryt), pp. 217–224. Springer-Verlag, Berlin.

Braithwaite, C.J.R. (1973) Settling behaviour related to sieve analysis of skeletal sands. *Sedimentology*, **20,** 251–262.

Cabral, A.P. (1993) Extração da batimetria e dos tipos de substrato de um setor da plataforma continental do Rio *Grande do Norte, utilizando imagens* TM-Landsat. *MSc thesis in Remote Sensing,* Instituto Nacional de Pesquisas Espaciais, São José dos Campos, Brazil.

Campos, C.W.M., Ponte, F.C. and Miura, K. (1974) Geology of the Brazilian continental margin. In: *The Geology of Continental Margins* (Ed. by C. A. Burk and C. L. Drake), pp. 447–461. Springer-Verlag, New York.

Carannante, G., Esteban, M., Milliman, J.D. and Simone, L. (1988) Carbonate lithofacies as palaeolatitude indicators: problems and limitations. *Sedim. Geol.*, **60,** 333–346.

Colombini, M. (1993) Turbulence-driven secondary flow formation of sand ridges. *J. Fluid Mech.*, **254,** 701–719.

Coutinho, P.N. (1981) Sedimentação na plataforma continental. Alagoas-Sergipe. *Arq. Ciênc. Mar.*, **21,** 1–18.

Cunha, E.M.S., Silveira, I.M., Nogueira, A.M.B. and Vilaça, J.G. (1990) Análise ambiental do setor

costeiro Maxaranguape-Touros, R.N. *Anais: Third Congresso Brasileiro de Geologia*, *Natal*, 770–795.
Drake, T.G., Shreve, R.L., Dietrich, W.E., Whiting, P.J. and Leopold, L.B. (1988) Bedload transport of fine gravel observed by motion-picture photography. *J. Fluid Mech.*, **192,** 193–217.
Emery, K.O. (1968) Relict sediments on continental shelves of the world. *Am. Assoc. Petrol. Geol.*, **52,** 445–464.
Emery, K.O. and Milliman, J.D. (1975) Suspended matter in surface waters: influence of river discharge and upwelling. *Anais: 28*, *Congresso Brasileiro de Geologia*, *Porto Alegre*, 225–235.
Farrow, G., Scoffin, T., Brown, B. and Cucci, M. (1979) An underwater television survey of facies variation on the inner Scottish shelf Colonsay, Islay and Jura. *Scot. J. Geol.*, **15,** 13–29.
Flemming, B.W. (1976) Side-scan sonar: a practical guide. *Int. Hydrog. Rev.*, **53,** 65–92.
Flemming, B.W. (1978) Underwater sand dunes along the southeast African continental margin – observations and implications. *Mar. Geol.*, **26,** 177–198.
Flemming, B.W. (1980) Sand transport and bedform patterns on the continental shelf between Durban and Port Elizabeth (southeast African continental margin). *Sedim. Geol.*, **26,** 179–205.
Flemming, B.W. (1988) Zur klassifikation subaquatischer, stromungstrans versaler transportkorper. *Bosh. Geol. U. Geotechn. Arb.*, **29,** 44–47.
Flemming, B.W. (1992) Bed phase in bioclastic sands exposed to unsteady non-equilibrium flows: an experimental flume study. *Senkenberg. Marit.*, **22,** 95–108.
Flood, R.D. (1983) Classification of furrow and a model for furrow initiation and evolution. *Geol. Soc. Am. Bull.*, **94,** 630–639.
Folk, R.L. and Ward, W.C. (1957) Brazos River Bar: a study in significance of grain size parameters. *J. Sedim. Petrol.*, **27,** 3–26.
França, A.M.C., Coutinho, P.N. and Summerhayes, C.P. (1976) Sedimentos superficiais da margem continental nordeste brasileira. *Rev. Bras. Geol.*, **6,** 71–89.
Hayes, M.O. (1979) Barrier island morphology as a function of tidal and wave regime. In: *Barrier Islands* (Ed. by S. P. Leathermann), pp. 1–27. Academic Press, New York.
Hine, A.C., Wilber, R.J. and Neumann, A.C. (1981) Carbonate sand bodies along contrasting shallow bank margins facing open seaway in Northern Bahamas. *Am. Assoc. Petrol. Geol. Bull.*, **65,** 261–290.
Holmes, N.A. and Wilson, J.B. (1985) Faunas associated with longitudinal furrows and sand ribbons in a tide-swept area in the English Channel. *J. Mar. Biol. Assoc. UK*, **65,** 10–51.
Jackson, II, R.G. (1975) Hierarchical attributes and unifying model of bedforms composed of cohesionless material and produced by shearing flow. *Geol. Soc. Am. Bull.*, **86,** 1523–1533.
Jell, J.S. and Maxwell, W.H. (1965) The significance of the larger foraminifera in the Heron Island reef sediments. *J. Paleontol.*, **39,** 273–279.
Kenyon, N.H. (1970) Sand ribbons of European tidal seas. *Mar. Geol.*, **33,** 25–39.
Komar, P.D. and Miller, M.C. (1973) The threshold of sediment movement under oscillatory water waves. *J. Sedim. Petrol.*, **43,** 1101–1110.
Kuijpers, A., Werner, F. and Rumohr, J. (1993) Sandwaves and other large-scale bedforms as indicators of non-tidal surge currents in the Skagerrak off northern Denmark. *Mar. Geol.*, **111,** 209–221.
Laborel, J. (1969) Les Peuplements de Madréporaires des cotes Tropicales du Brésil. *Ann. l'Univ. D'Abid Série E*, **2** (3), 1–261.
Mabesone, J.M. and Coutinho, P.N. (1970) Littoral and shallow marine geology of northern and northeastern Brazil. Universidade Fedederal de Pernambuco. *Trab. Ocean*, **12,** 214.
MacCave, I.N. (1971) Sand waves in the North Sea off the coast of Holland. *Mar. Geol.*, **10,** 199–225.
McLean, S.R. (1981) The role of non-uniform roughness in the formation of sand ribbons. *Mar. Geol.*, **42,** 49–74.
McManus, J. (1988) Grain size determination and interpretation. In: *Techniques in Sedimentology* (Ed. by M. Tucker), pp. 63–85. Blackwell Scientific Publications, Oxford.
Maiklem, W.R. (1968) Some hydraulic properties of bioclastic carbonate grains. *Sedimentology*, **10,** 101–109.
Molinari, R.L., Garzoli, S.L., Katz, E.G., Harrison, D.E., Richardson, P.L. and Reverdin, G. (1986) A synthesis of the first GARP global experiment (FGGE) in the Equatorial Atlantic Ocean. *Proc. Ocean.*, **16,** 91–112.
Oliveira, M.I.M., Bagnoli, E., Farias, C.C., Nogueira, A.M.B. and Santiago, C. (1990) Considerações sobre a geometria, petrografia, sedimentação, diagenese e idade dos beachrocks do Rio Grande do Norte. *Anais: 36th Congresso Brasileiro de Geologia*, *Natal*, **2,** 769–783.
Pantin, H.M. (1991) The sea-bed sediments around the United Kingdom. Their bathymetric and physical environment, grain size, mineral composition and associated bedforms. *Br. Geol. Surv., Res. Rep. SB/90/1. Offshore Geol. Series.*
Pantin, H.M., Hamilton, D. and Evans, C.D.R. (1981) Secondary flow caused by differential roughness, Langmuir circulations, and their effect on the development of sand ribbons. *Geol. Mar. Lett.*, **1,** 255–260.
Peterson, R.G. and Stramma, L. (1991) Upper-level circulation in the South Atlantic Ocean. *Proc. Ocean.*, **20,** 1–73.
Prager, E.J., Southard, J.B. and Vivoni-Gallart, E.R. (1996) Experiments on entrainment threshold of well-sorted and poorly sorted carbonate sands. *Sedimentology*, **43,** 33–40.
Rao, V.B., Lima, M.C. and Franchito, S.H. (1993) Seasonal and interannual variations of rainfall over eastern northeast Brazil. *J. Climate*, **6,** 1754–1763.
Richardson, P.L. and Walsh, D. (1986) Mapping climatological seasonal variation of surface currents in the Tropical Atlantic using ship drifts. *J. Geophys. Res.*, **91,** 10537–10550.

Schultz, P., Barron, E.J., Sloan, II, J.L. (1992) Assessment of NCAR general circulation model precipitation in comparison with observations. *Palaeogeogr., Palaeoclimatol., Palaeoecol. (Global Plan. Chan.)*, **97,** 269–310.

Servain, J., Séva, M., Lukas, S. and Rougier, G. (1987) Climatic atlas of the tropical Atlantic wind stress and surface temperature: 1980–84. *Ocean-Air Int.*, **1,** 109–182.

Servain, J., Séva, M. and Rual, P. (1990) Climatological comparison and long-term variations of sea surface temperature over the tropical Atlantic Ocean. *J. Geophys. Res.*, **95,** 9421–9431.

Shinn, E.A., Lidz, B. and Holmes, C.W. (1990) High-energy carbonate-sand accumulations, the Quicksands, southwest Florida Key. *J. Sedim. Petrol.*, **60,** 952–967.

da Silveira, I.C.A., de Miranda, L.B. and Brown, W.S. (1994) On the origins of the North Brazil Current. *J. Geophys. Res.*, **99,** 22501–22512.

Solewicz, R. (1989) *Feições fisiográficas submarinas da plataforma continental do Rio Grande do Norte visíveis por imagen de satélite*. MSc thesis, Instituto Nacional de Pesquisas Espaciais, São José dos Campos, Brazil.

Sorokina, N.A. (1984) Distribution of the transparency of water in the tropical Atlantic. *Oceanology*, **24,** 58–60.

Southard, J.B. and Boguchwal, L.A. (1973) Flume experiments on the transition from ripples to lower flat bed with increasing sand size. *J. Sedim. Petrol.*, **43,** 1114–1121.

Srivastava, N.K. and Corsino, A.R. (1984) Os carbonates de Touros, petrografia e estratigrafia. *Anais: 11, Simpósio de Geologia do Nordeste, Natal, Brazil*. 165–176.

Steidtmann, J.R. (1982) Size-density sorting of sand-size spheres during deposition from bedload transport and implications concerning hydraulic equivalence. *Sedimentology*, **29,** 877–883.

Stramma, L., Ikeda, Y. and Peterson, R.G. (1990) Geostrophic transport in the Brazil current region north of 20°S. *Deep-Sea Res.*, **37,** 1875–1886.

Stride, A.H. (1970) Shape and size trends for sand waves in a depositional zone of the North Sea. *Geol. Mag.*, **107,** 469–477.

Stride, A.H. (ed.) (1982) *Offshore Tidal Sands*. Chapman & Hall, London.

Tchernia, P. (1980) *Descriptive Regional Oceanography*. Pergamon Marine Series, Oxford.

Terhorst, A. (1988) *The Seafloor Environment o Simon's Town in False Bay, Revealed by Side-Scan Sonar, Bottom Sampling, Diver Observation and Underwater Photography*. Joint Geological Survey/University of Cape Town, *Mar. Geosci. Unit Bull.*, **22**.

Testa, V. (1996) *Quaternary Sediments of the Shallow Shelf, Rio Grande do Norte, NE Brazil*. PhD thesis, University of London.

Testa, V. (1997) Calcareous algae and corals in the inner shelf of Rio Grande do Norte, NE Brazil. *Proc. 8th Int. Coral Reef Symp. Panama*, **1,** 737–742.

Testa, V. and Bosence, D.W.J. (1998) A distally steepened, high energy, tropical ramp from the northeast Brazilian shelf. In: *Carbonate Ramps: Oceanographic and Biological Controls, Modelling and Diagenesis* (Ed. by V. P. Wright and T. P. Burchette), *Geol. Soc. Lond. Spec. Publ.*, **149**, 55–71.

Testa, V., Gherardi, D.M., Bosence, D.W.J. and Vianna, M.L. (1994) Tropical algal carbonates from shelf and offshore atoll environments, Northeast Brazil. *Abstracts 14th Int. Sedimentological Congress, Recife*. B17–B18.

Testa, V., Bosence, D.W.J. and Vianna, M.L. (1997) Submerged lithologies as indicators of relative sea-level oscillations in Rio Grande do Norte, NE Brazil. *Proc. 4th Cong. Brasileiro de Estudos do Quaternario,* 155–160.

Vianna, M.L., Solewicz, R., Cabral, A. and Testa, V. (1991) Sandstream on the northeast Brazilian Shelf. *Cont. Shelf Res.*, **2,** 509–524.

Vianna. M.L., Cabral, A.P. and Gherardi, D.M. (1993) TM-Landsat imagery to the study of the impact of global climate change on a tropical environment during the last deglaciation. *Int. J. Remote Sensing*, **14,** 2971–2983.

Werner, F. and Newton, R.S. (1975) The pattern of large-scale bed forms in the Langeland belt (Baltic Sea). *Mar. Geol.*, **33,** 29–59.

Wiekman, B.E., Wimbush, M. and Van Leer, J.C. (1989) Secondary circulation in the boundary layer over sedimentary furrows. *J. Geophys. Res.*, **94,** 9721–9730.

Wilson, J.B. (1979) Biogenic carbonate sediments on the Scottish continental shelf and on Rockall Bank. *Mar. Geol.*, **33,** M85–M93.

Wilson, J.B. (1982) Shelly faunas associated with temperate offshore tidal deposits. In: *Offshore Tidal Sands* (Ed. by A. H. Stride), pp. 126–171. Chapman & Hall, London.

Wilson, J.B. (1986) Faunas on tidal currents and wave-dominated continental shelves and their use in the recognition of storm deposits. In: *Shelf Sands and Sandstones* (Ed. by R. J. Knight and J. R. McLean), *Can. Soc. Petrol. Geol. Mem.*, **II,** 313–326.

Wilson, J.B. (1988) A model for temporal changes in the faunal composition of shell gravels during a transgression on the continental shelf around the British Isles. *Sedim. Geol.*, **60,** 95–105.

Manuscript received 10 May 1996;
revision accepted 7 May 1998.